第 26 卷第 4 期 无 机 化 学 学 报 Vol.26 No.4
2010 年 4 月 CHINESE JOURNAL OF INORGANIC CHEMISTRY 573-580

一维纳米 Co_3O_4,Ag/Co_3O_4 及 CuO/Co_3O_4 的合成与电催化性能

潘 路[1,2] 张祖德*,[1]
([1] 中国科学技术大学化学系,合肥 230026)
([2] 淮南师范学院化学与化工系,淮南 232001)

摘要: 采用水热合成法制备了 Co_3O_4 及复合 Ag/Co_3O_4、CuO/Co_3O_4 一维纳米产品。用 XRD,FE-SEM 和 TEM 手段对产品进行了表征。采用循环伏安法研究了合成产品修饰的玻碳电极在碱性溶液中对对硝基苯酚的电催化还原性能。与裸玻碳电极相比,1 mmol·L^{-1} 的对硝基苯酚在用 Co_3O_4、特别是 CuO/Co_3O_4 修饰的玻碳电极上还原的峰电流明显增大,用 Ag/Co_3O_4(Ag/Co 原子比分别为 1:5 和 2:5)修饰的玻碳电极催化还原对硝基苯酚时,尽管还原峰电流增大不是太大,但其峰电位明显降低(分别降低 0.265 和 0.371 V)。

关键词: Co_3O_4; Ag/Co_3O_4; CuO/Co_3O_4; 电催化; 对硝基苯酚
中图分类号: O614.81+2; O614.121; O614.122 **文献标识码**: A **文章编号**: 1001-4861(2010)04-0573-08

Synthesis and Electrocatalytic Property of One-Dimensional Nano-Co_3O_4, Ag/Co_3O_4 and CuO/Co_3O_4

PAN Lu[1,2] ZHANG Zu-De[1]
([1]*Department of Chemistry, University of Science and Technology, Hefei* 230026)
([2]*Department of Chemistry and Chemical Engineering, Huainan Normal University, Huainan, Anhui* 232001)

Abstract: One-dimensional Co_3O_4 as well as composite Ag/Co_3O_4 and CuO/Co_3O_4 products were synthesized via a hydrothermal method. The as-prepared samples were characterized by XRD, field emission scan electron microscopy (FE-SEM) and TEM techniques. The electrocatalytic properties for *p*-nitrophenol reduction in a basic solution using a glassy carbon electrode(GCE) modified with the as-synthesized samples were determined utilizing cyclic voltammetry method. Compared to a bare GCE, 1 mmol·L^{-1} p-nitrophenol could be reduced with an obviously larger peak current values on the GCE modified with Co_3O_4, especially with CuO/Co_3O_4 samples. Although the increase in the reduction peak current value is not very high in the case of Ag/Co_3O_4 modified GCEs with n_{Ag}/n_{Co} ratio of 1∶5 and 2∶5, respectively, *p*-nitrophenol could be reduced at the lower potential(the decrease in reduction peak potential is about 0.265 and 0.371 V, respectively).

Key words: Co_3O_4; Ag/Co_3O_4; CuO/Co_3O_4; electrocatalysis; p-nitrophenol

Nanosized transition metal oxides often exhibit enhanced chemical, physical, thermal, electrical, optical, or magnetic properties, thus finding extensive applications in electrochemistry, biomedical device and other fields[1-2]. Co_3O_4, an intrinsic p-type semiconductor (direct optical bandgaps at 1.48 and 2.19 eV)[3], has been investigated as a promising material in gas-sensing, solar energy absorption and as an effective

收稿日期:2009-11-25。收修改稿日期:2010-01-25。
*通讯联系人。E-mail:zhzude@163.com
第一作者:潘 路,男,39 岁,博士研究生;研究方向:无机材料的合成与性质研究。

catalyst in environmental purification and chemical engineering [4-5]. Much effort has been devoted to the fabrication of well-arranged nanostructure patterns, especially the arrangement of one-dimensional nanostructures because of their interesting physical properties and potential applications in many areas, such as in nanoelectronic and optoelec-tronic devices [6-8]. However, the report about the synthesis of single-crystal Co_3O_4 nanotubes or nanorods is scarce. Only a few reports on the synthesis of one-dimensional Co_3O_4 are available[9].

Silver particles have applications in catalysis, conductive inks, thick film pastes and adhesives for various electronic components, in photonics and photography [10-11]. Due to the excellent conductive performances of silver particles, a composite nanostructure composed of silver and metal oxide semiconductor may exhibit marvelous properties. Lai et al[12] reported that Ag/Fe_3O_4 exhibited superparamagnetic behavior at the temperature higher than the blocking temperature(373 K) and showed shifted loops under a field cooling process. In this work, Ag/Co_3O_4 nanomaterals with silver covered on Co_3O_4 nanotubes were fabricated via an easily controlled hydrothermal method. Cu-M(transition metals) composite oxides have been studied extensively as catalysts for CO oxidation, such as $CuO\text{-}CeO_2$[13-14], $CuO\text{-}Co_3O_4$[15], and $CuO\text{-}TiO_2$[16]. Cu-Co composite oxides have been investigated as anode for lithium-ion batteries in addition to the application as a catalyst for CO oxidation [17-18]. To the best of our knowledge, there have been few reports involving in the synthesis of one-dimensional CuO/Co_3O_4 materials, and the work on the electrocatalytic performances of Cu-Co composite oxides. In this work, one-dimensional Cu-Co composite oxides were also synthesized via an easily controlled and inexpensive method. The electrocatalytic activities for *p*-nitrophenol reduction with the one-dimensional Co_3O_4, Ag/Co_3O_4 nanotubes, and CuO/Co_3O_4 nanorods decorated on a GCE were tested, and the electrocatalytic activities for *p*-nitrophenol reduction were enhanced greatly with the modified GCE than that using a bare GCE in a basic solution.

1 Experimental

1.1 Synthesis of Co_3O_4 and Ag/Co_3O_4 samples

The precursor of Co_3O_4 was prepared via a hydrothermal procedure. Typically, 2.5 mmol of $CoCl_2\cdot 6H_2O$, 5 mmol of sodium tartrate, 10 mmol of urea, and 0.5 g of PEG-6000 were dissolved in 40 mL of distilled water to obtain a homogeneous solution, then the solution was transferred to 60 mL of Teflon-lined stainless steel autoclave. The autoclave was sealed and maintained at 180 ℃ for 16 h in a digital-temperature-controlled oven and then cooled to room temperature naturally. A pink precipitate thus obtained was filtered out and washed with distilled water then ethanol for several times, and dried in vacuum at 80 ℃ for 6 h. The Co_3O_4 sample was obtained by calcination of the precursor at 400 ℃ for 3 h according to the TG analysis of the Co_3O_4 precursor. To obtain Ag/Co_3O_4, a certain amount of Co_3O_4 sample was dispersed in 30 mL of distilled water under supersonication conditions, then the desired amount of $Ag(NH_3)_2^+$ and 2 mL of triethanolamine were added and the supersonic treatment was undergone for 30 min, finally the content was transferred to 60 mL of Teflon-lined stainless steel autoclave. The autoclave was sealed and maintained at 120 ℃ for 12 h and then cooled to room temperature naturally. The black precipitate obtained was centrifuged and washed with distilled water then ethanol for several times, and dried in vacuum at 50 ℃ for 6 h.

1.2 Synthesis of CuO/Co_3O_4 samples

To synthesize CuO/Co_3O_4 products, the corresponding precursors were synthesized first via a co-precipitation procedure then a hydrothermal method. Typically, 5 mmol of $CoCl_2\cdot 6H_2O$ and 2.5 mmol of $CuSO_4\cdot 5H_2O$ were dissolved in 15 mL distilled water, then 25 mL 0.32 $mol\cdot L^{-1}$ $(NH_4)_2C_2O_4$ solution was added dropwise under vigorous stirring, subsequently 1.25, 2.5 or 5 mL of cycolohexylamine was added and the mixed system was transferred to 60 mL of Teflon-lined stainless steel autoclave, which was treated at 120 ℃ for 12 h. Finally a grey precipitate was filtered and washed with distilled water then ethanol for several

times, and dried in vacuum at 80 ℃ for 8 h. By calcining the precursors at 400 ℃ for 3h based on the TG analysis, the resulting CuO/Co_3O_4 products were prepared.

1.3 Characterization

The phase analysis of the as-synthesized products was examined by a Philips XPert PROSUPER X-Ray powder diffractometer(XRD) with Cu $K\alpha$ radiation(λ = 0.154 18 nm), using an operation voltage and current of 40 kV and 40 mA. The SEM images were carried on a JEOL-6300F Field-emission scan electron microscopy (FE-SEM) with an accelerating voltage of 15 kV. The TEM images were collected on a Hitachi Model H-800 transmission electron microscopy, using an accelerating voltage of 200 kV. N_2 adsorption of the as-prepared samples was determined by BET measurements using a NOVA-1000e surface analyzer.

1.4 Electrochemical property measurement

The electrochemical property measurements of a GCE decorated with the as-prepared products was performed on LK 98 microcomputer-based electrochemical system. A three-electrode single compartment cell was used for cyclic voltammetry. A GCE(3.7 mm diameter) was used as working electrode and a platinum plate used as counter electrode and a Ag/AgC1 electrode used as reference electrode. Prior to each measurement, the GCE surface was carefully polished on an abrasive paper first, then further polished with 0.3 and 0.05 μm α-Al_2O_3 (Buehler) paste in turn, finally rinsed thoroughly with 1∶1(V/V) HNO_3 aqueous solution, acetone and doubly distilled water and dried in air. A 20 mg sample was dispersed in 4 mL doubly distilled water under ultrasonication to obtain a black suspension solution. Of the as-prepared solution, 50 μL was taken out and trickled on the carbon surface of the GCE. After being dried in air, the modified GCE was prepared and used directly for electrochemical measur ements.

2 Results and discussion

Fig.1 shows typical SEM images of the as-synthesized precursors of Co_3O_4 and CuO/Co_3O_4. From Fig.1a, it can be seen that the precursor of Co_3O_4 represents rod-like morphology, but it is composed of numerous rods with non-uniform lengths. As can be seen from Fig.1b, the precursor of CuO/Co_3O_4 is composed of uniform rod-like structures with diameter about 500 nm and length approximately of 5 μm.

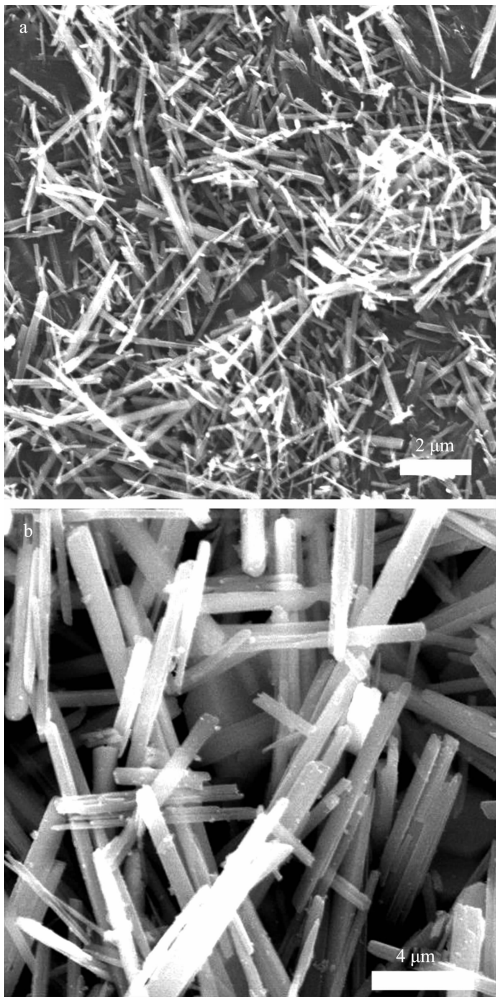

Fig.1　SEM images of the precursor of (a) Co_3O_4 and (b) CuO/Co_3O_4 prepared with addition of 2.50 mL of cyclohexylamine

Fig.2 shows the XRD patterns of as-prepared Co_3O_4, Ag/Co_3O_4 and CuO/Co_3O_4 composites. From Fig. 2a, the diffraction patterns demonstrate that the sample consists of cubic Co_3O_4 phase. As can be seen from Fig.2b and c, cubic Ag phase and cubic Co_3O_4 phase are clearly evidenced, indicating the formation of Ag/Co_3O_4 composites. The diffraction intensity of Ag phase becomes stronger with increasing of Ag in the composites. Compared to Fig.2d to g, CuO and Co_3O_4 phases could be detected in Fig.2d to f, however, only diffraction peaks ascribed to the spinel phase of Co_3O_4

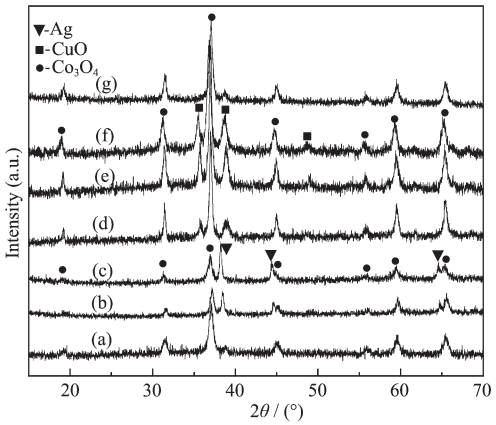

Fig.2 XRD patterns of (a) Co_3O_4, (b) Ag/Co_3O_4 with Ag/Co atomic ratio of 1:5, (c) Ag/Co_3O_4 with Ag/Co atomic ratio of 2:5, CuO/Co_3O_4 samples prepared with addition of (d) no cyclohexylamine, (e) 1.25 mL of cyclohexylamine, (g) 2.50 mL of cyclohexylamine (f), and 5.00 mL of cyclohexylamine

can be observed in Fig.2g. Thus the addition of cyclohexylamine has a significant effect on the phases of samples. With addition of 0, 1.25 and 2.50 mL of cyclohexylamine, both CuO and Co_3O_4 phases appears (Fig.2d, e and f), but as the addition amount of cyclohexylamine reaches to 5.00 mL, the strong diffraction peaks only ascribed to the spinel phase of Co_3O_4 could be observed distinctly, and nearly no diffraction peaks ascribed to monoclinlic tenorite structure of CuO phase could be detected(Fig.2g). Co_3O_4 can be described by a formula unit AB_2O_4(A→Co^{2+}, B→Co^{3+}) and exhibits a normal spinel crystal structure with occupation of tetrahedral A sites by Co^{2+} and octahedral B sites by Co^{3+} in cubic closely-packed structure of O^{2-}, where the ratio of $n_{Co^{3+}}/n_{Co^{2+}}$ is 2:1 [19]. As Cu^{2+} possess the ionic charge and similar ionic diameter($D_{Cu(Ⅱ)}$=73 pm) to Co^{2+} ($D_{Co(Ⅱ)}$=74.5 pm), it is reasonable to speculate that Cu^{2+} could replace Co^{2+} entering the cubic structure of Co_3O_4, and a composite spinel structure of $Cu_xCo_{3-x}O_4$ could be formed[15]. If Co^{2+} in Co_3O_4 is replaced totally by Cu^{2+}, the maximum number of Cu^{2+} accommodated by $Cu_xCo_{3-x}O_4$ with spinel structure is at n_{Cu}/n_{Co} ratio of 1:2. As mentioned in the experimental section, for the synthesis of CuO/Co_3O_4 samples, the Cu/Co atomic ratio was controlled at 1:2, and the excessive cyclohexylamine possibly is advantageous to form co-complex precursor of Cu(Ⅱ) and Co(Ⅱ). By calcination of the precursor, $CuCo_2O_4$ with spinel structure is formed.

The TEM images of Co_3O_4 and composite Ag/Co_3O_4 are observed clearly in Fig.3. The Co_3O_4 represents uniform tube-like structure (Fig.3a). It is found that PEG plays a significant role on the fabrication of Co_3O_4 nanotubes. Without addition of PEG for synthesis of the precursor of Co_3O_4, only irregular Co_3O_4 rods could be prepared by calcination of the precursor at 400 ℃ for 3 h(Fig.3b). Fig.3c and d display the TEM images of composite Ag/Co_3O_4 with n_{Ag}/n_{Co} ratio of 1:5 and 2:5, respectively. It can be seen that Ag particles are covered on the walls of Co_3O_4 tubes. With increasing the amount of Ag in the composites, more Ag particles with less size are covered on the walls of Co_3O_4 tubes.

Fig.4 shows the FE-SEM images of CuO/Co_3O_4 products prepared with addition of different volumes of cyclohexylamine. The samples represent rod-like morphologies shown in Fig.4a~c, but the one displaying in Fig.4d exhibits belt-like morphology. Obviously, the addition of different volumes of cyclohexylamine plays

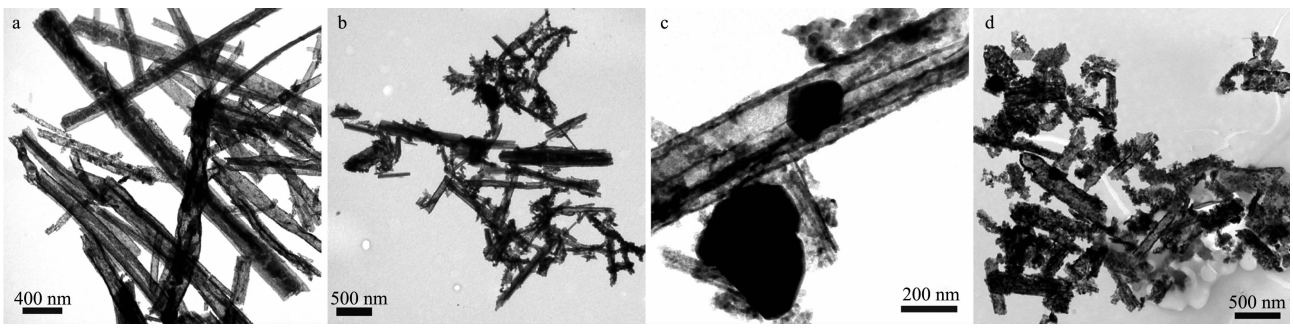

Fig.3 TEM images of samples Co_3O_4 prepared with addition of PEG (a) and without addition of PEG (b). TEM images of Ag/Co_3O_4 with n_{Ag}/n_{Co} ratio of 1:5 (c) and 2:5 (d)

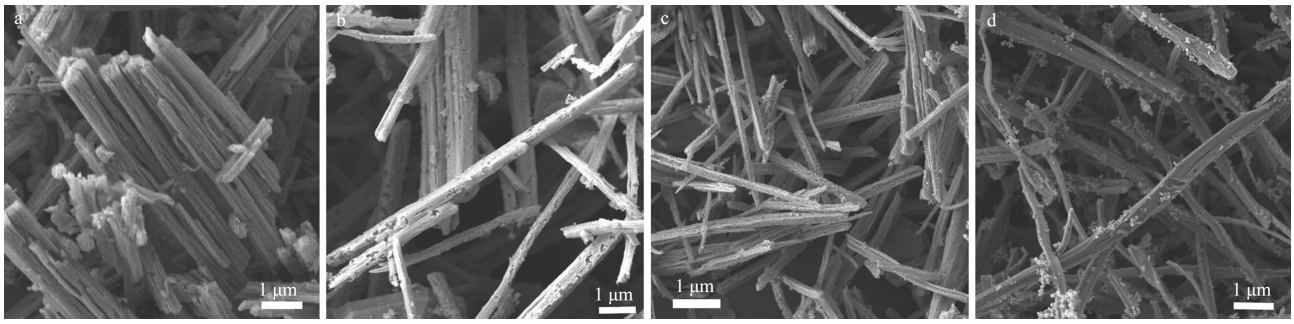

(a) without addition of cyclohexylamine, (b), (c) and (d), with addition of 1.25 mL, 2.50 mL and 5.00 mL of cyclohexylamine, respectively.

Fig.4　FE-SEM images of the as-prepared CuO/Co_3O_4 samples

an important role on the morphologies of the final products. Without addition of cyclohexylamine, the sample mainly displays rod-like morphology, but the rods are nonuniform, furthermore a few particles could be detected (Fig.4a). With addition of 1.25 mL cyclohexylamine, the rods are uniform and a few caves in the rods can be observed(Fig.4b). By increasing the volume of cyclohexylamine to 2.50 mL, the rods become more uniform and thinner, and a few belt-like CuO/Co_3O_4 appears(Fig.4c). Further increasing the volume of cyclohexylamine to 5.00 mL, the sample takes on belt-like structure, and nearly no rod-like morphology can be detected(Fig.4d).

Fig.5 shows the TEM images of the as-prepared CuO/Co_3O_4 samples synthesized with the addition of different volumes of cyclohexylamine. The image shown in Fig.5a corresponds to the sample prepared without addition of cyclohexylamine, and the sample shows rod-like morphology, in good agreement with the FE-SEM image shown in Fig.4a. Fig.5b and c exhibit the TEM images of the CuO/Co_3O_4 sample prepared with addition of 2.50 mL cyclohexylamine. From Fig.5b, the surfaces of the rod-like sample are smooth and its mean diameter is about 300 nm. According to Fig.5c, the rod is composed of a great deal of particles. Based on the SEM and TEM images, it can be concluded reasonably that cyclohexylamine is advantageous in directing the precursor of CuO/Co_3O_4 to grow along one-dimensional direction. By calcining the precursor, Cu(Ⅱ) and Co(Ⅱ) oxalates or Cu(Ⅱ) and Co(Ⅱ) complex decompose to form metal oxides or $CuCo_2O_4$ particles, and the samples maintain one-dimensional arrangement.

Cyclic voltammogrames of a bare GCE in absence and presence of *p*-nitrophenol and the GCE modified with Co_3O_4, Ag/Co_3O_4 and CuO/Co_3O_4 samples in presence of *p*-nitrophenol in a basic solution are shown in Fig.6 and 7. When a bare GCE is used, *p*-nitrophenol reduction is carried out only with a current peak value of 40 μA at a potential of −1.044 V, as curves(2) shown in Fig.6 and 7, the peak current is lower and the peak potential is higher, suggesting that the bare GCE exhibits poor electrocatalytic activity for *p*-nitrophenol reduction under the condition. When the GCE is decorated with the as-prepared one-dimensional samples, namely with Co_3O_4, Ag/Co_3O_4 and CuO/Co_3O_4, the modified GCEs exhibit different catalytic activities

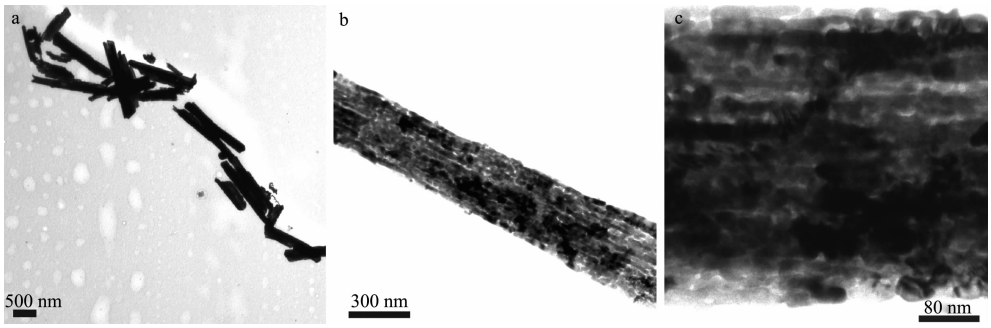

(a) without addition of cyclohexylamine, (b) with addition of 2.50 mL of cyclohexylamine, (c) magnified TEM image of (b)

Fig.5　TEM images of CuO/Co_3O_4 samples

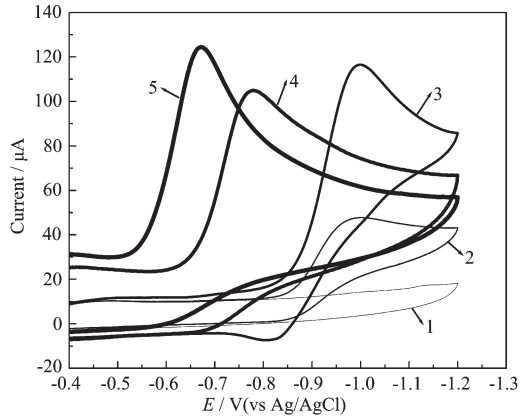

(1) in 1.0 mol·L^{-1} sodium hydroxide and a bare GCE, (2) in 1.0 mol·L^{-1} sodium hydroxide +1.0 mmol·L^{-1} *p*-nitrophenol, a glassy GCE modified with Co_3O_4, (3) Ag/Co_3O_4 with Ag/Co atomic ratio of 1:5, (4) and Ag/Co_3O_4 with Ag/Co atomic ratio of 2:5, (5) in 1.0 mol·L^{-1} sodium hydroxide +1.0 mmol·L^{-1} *p*-nitrophenol (scan rate 0.02 V·s^{-1})

Fig.6 Cyclic voltammorgrams of a bare glassy carbon electrode (GCE)

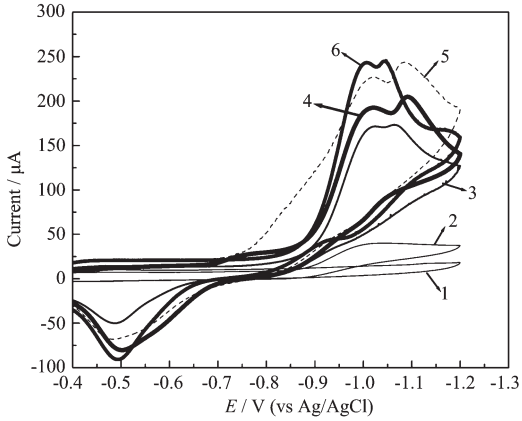

(1) in 1.0 mol·L^{-1} sodium hydroxide and a bare glassy carbon electrode (2) in 1.0 mol·L^{-1} sodium hydroxide +1.0 mmol·L^{-1} *p*-nitrophenol, GCE modified with CuO/Co_3O_4 prepared without addition of cyclohexylamine (3), with addition of 1.25 mL of cyclohexylamine (4) 2.50 mL of cyclohexylamine (5) with addition of 5.00 mL of cyclohexylamine (6) in 1.0 mol·L^{-1} sodium hydroxide +1.0 mmol·L^{-1} *p*-nitrophenol(scan rate 0.02 V·s^{-1})

Fig.7 Cyclic voltammorgrams of a bare glassy carbon electrode(GCE)

for *p*-nitrophenol reduction. As can be seen from the curve (3), (4) and (5) in Fig.6, *p*-nitrophenol is reduced with the peak current values of 116, 105 and 124 μA at the potential of −1.001, −0.779 and −0.673V using the GCE modified with Co_3O_4, Ag/Co_3O_4 with n_{Ag}/n_{Co} ratio of 1:5, and Ag/Co_3O_4 with n_{Ag}/n_{Co} ratio of 2:5, respectively. Compared to the peak current value with a bare GCE, p-nitrophenol reduction is carried out with 2.9, 2.6, and 3.1 times larger peak current values using the three modified GCEs respectively. Though *p*-nitrophenol could be reduced with a higher peak current using the GCE modified with tube-like Co_3O_4, the peak potential is rather higher. However, the reduction peak potential decreases about 0.265 V and 0.371 V using the GCE modified with one-dimensional Ag/Co_3O_4 samples with n_{Ag}/n_{Co} ratio of 1:5 and 2:5, respectively. Clearly, the Ag/Co_3O_4 modified GCE with n_{Ag}/n_{Co} ratio of 2:5 exhibits a better catalytic activity for *p*-nitrophenol reduction than the Ag/Co_3O_4 modified one with n_{Ag}/n_{Co} ratio of 1:5 at lower potential, e.g. the current values are 25 and 31 μA, respectively, with the Ag/Co_3O_4 modified GCE samples with n_{Ag}/n_{Co} ratio of 1:5 and 2:5 when the potential is fixed at −0.400 V. We synthesized the Ag/Co_3O_4 samples with higher n_{Ag}/n_{Co} ratios, e.g. 2.5:5 and 3:5, and they are used as the catalysts for *p*-nitrophenol reduction at the same conditions. The results reveal that the catalysts have poor stability and repeatability.

From Fig.7, the CuO/Co_3O_4 modified GCEs samples prepared with addition of 0, 1.25, 2.50 and 5.00 mL of cyclohexylamine, respectively, all show higher catalytic activity for *p*-nitrophenol reduction as seen from curve(3), (4), (5) and (6), respectively. Using the four modified GCEs, there are two obvious reduction peaks appearing at the potential in the range of −0.9 to −1.1 V. At lower peak potentials, the four reduction peak potential values basically keep constant, i.e. at −1.026, −1.020, −1.020 and −1.007 V, and the corresponding peak current values are as high as 171, 192, 227 and 243 μA, respectively. Compared to the peak current value with a bare GCE, *p*-nitrophenol reduction is carried out with 4.3, 4.8, 5.7 and 6.1 times larger peak current values using the four modified GCEs, respectively. Obviously, the CuO/Co_3O_4 samples prepared with addition of different volumes of cyclohexylamine exhibit different catalytic activities for *p*-nitrophenol reduction. By increasing the addition volume of cyclohexylamine from 0 to 5.00 mL, the catalytic activity of the as-prepared CuO/Co_3O_4 sample

increases. Additionally, the sample prepared with the addition of 2.50 mL of cyclohexylamine shows a higher catalytic activity for p-nitrophenol reduction at lower potential than the other three samples, e.g. the current value is 85 μA using the corresponding modified GCE while the current values are 22, 34 and 31 μA using the other three CuO/Co_3O_4 modified GCEs samples prepared with the addition of 0, 1.25 and 5.00 mL cyclohexylamine, respectively, at the potential of −0.80 V. It also could be seen that the each oxidation peak current appeared in curve (3), (4), (5) and (6) is about in the range of −0.44 to −0.54 V, namely, the four CuO/Co_3O_4 samples also exhibit a certain catalytic activity for p-nitrophenol oxidation at lower potential in a basic solution. However, the oxidation current basically disappears when the potential is over −0.7 V. As mentioned the above, there are two obvious reduction peak currents with the four modified GCEs, indicating a more complicate reduction mechanism.

To investigate the effect of scan rate on the electrocatalytic activity, the GCE modified with Ag/Co_3O_4 samples with n_{Ag}/n_{Co} ratio of 2∶5 was used. Fig.8a shows the cyclic voltammograms of the modified GCE electrode for *p*-nitrophenol reduction by increasing scan rate(υ). The peak current(I_{pc}) of *p*-nitrophenol reduction (Fig.8b) increases linearly with the square root of scan rate from 0.01 −0.1 V·s^{-1}, indicating *p*-nitrophenol reduction on theAg/Co_3O_4/GCEs attributes to diffusion-controlled reaction[20]. The further experiments indicated that *p*-nitrophenol reduction on the GCE modified with other samples basically is pertinent to diffusion-controlled procedure.

Based on the above experiments, the modified GCEs have revealed higher electrocatalytic activity for *p*-nitrophenol reduction by comparing to a bare GCE. *p*-nitrophenol can be reduced efficiently on the Ag/Co_3O_4 modified GCE at lower potentials (peak potential between −0.6 and −0.8 V), however, it only can be reduced efficiently on the CuO/Co_3O_4 modified one at higher potentials (peak potential between −0.95 and −1.2 V). The different catalytic activities may be attributed to their special structures. The specific surface area of Co_3O_4 and Ag/Co_3O_4 with n_{Ag}/n_{Co} ratio of

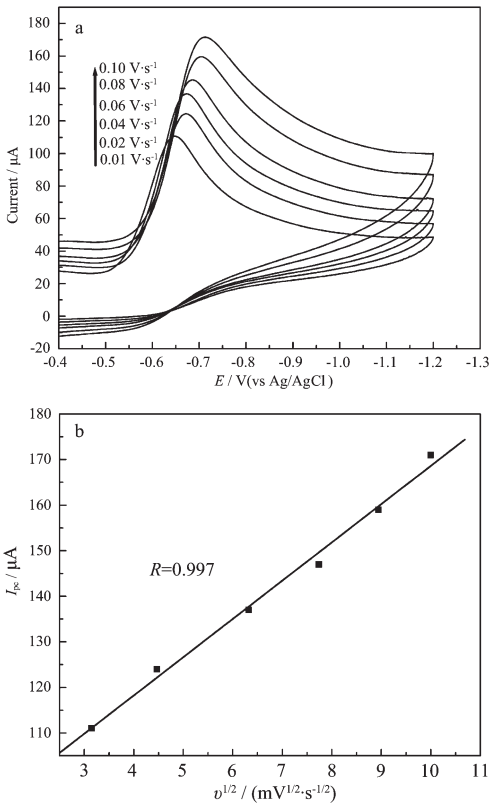

Fig.8　Cyclic voltammograms of a GCE modified with Ag/Co_3O_4 Ag/Co_3O_4 with n_{Ag}/n_{Co} ratio of 2∶5 at different scan rate (a) and the plot of I_{pc} vs. square root of scan rate (b) in 1.0 mol·L^{-1} sodium hydroxide +1.0 mmol·L^{-1} *p*-nitrophenol

2∶5 is 63 and 53 m^2·g^{-1}, but the one of CuO/Co_3O_4 (preparation with addition of 2.5 mL cyclohexylamine) is only 22 m^2·g^{-1}. The BET surface area of Ag/Co_3O_4 decreases because of insetting of aggregated Ag atoms on the Co_3O_4 nanotubes, but the electrocatalytic activity for *p*-nitrophenol reduction enhances greatly, which may be attributed to Ag atom revealing higher catalytic activity. Ag has empty 5*p* orbitals and may combine with *p*-nitrophenol to form intermediary compounds, which facilitates to lower the reaction activity energy. For the CuO/Co_3O_4 samples, the electrocatalysis reduction of *p*-nitrophenol may be related to transferring of the electrons between Cu(Ⅱ), Co(Ⅱ) and Co(Ⅲ). At larger negative potential, Cu(Ⅱ) and Co(Ⅲ) may be reduced to Cu(Ⅰ) and Co(Ⅱ) first, then *p*-nitrophenol can be reduced by the Cu (Ⅰ) and Co(Ⅱ), and Cu (Ⅰ) and Co(Ⅱ) are converted into Cu(Ⅱ) and Co(Ⅲ). Possibly Cu(Ⅱ) and Co(Ⅲ) have a certain synergic catalysis for the *p*-

nitrophenol reduction, the exact mechanism shall be studied in the future work.

3 Conclusions

One-dimensional pre cursors of Co_3O_4 and CuO/Co_3O_4 were prepared via an easily controlled hydrothermal method. Co_3O_4 nanotubes were obtained by calcining the precursors at 400 ℃ for 3 h. Silver particles were covered on the walls of Co_3O_4 nanotubes by the reduction of triethanolamine via a hydrothermal procedure at 120 ℃ for 12 h. PEG plays an important role in the synthesis of Co_3O_4 nanotubes. Without addition of PEG, only irregular Co_3O_4 rods could be obtained. The morphologies and sizes of CuO/Co_3O_4 products are influenced significantly by the addition of cyclohexylamine. By addition of 0, 1.25 and 2.50 mL of cyclohexylamine, CuO/Co_3O_4 rods could be fabricated. Further increasing the volume of cyclohexylamine to 5.00 mL, CuO/Co_3O_4 belts could be obtained. The as-prepared Co_3O_4, Ag/Co_3O_4 and CuO/Co_3O_4 products decorated on a GCE, respectively, were used to reduce *p*-nitrophenol. The results indicate compared to on a bare GCE, p-nitrophenol could be reduced with a higher peak current value but at an invariable peak potential on the Co_3O_4 and CuO/Co_3O_4 modified GCE samples, however it could be carried out at a lower peak potential. As a whole, the as-synthesized samples all show higher electrocatalytic activities for *p*-nitrophenol reduction in a basic solution.

References:

[1] Xu C, Teja A. *J. Supercrit. Fluids*, **2008**,**44**:85-91

[2] Cantalini C, Post M, Buso D, et al. *Sens. Actuators B*, **2005**, **108**,184-192

[3] Gulino A, Fiorito G, Fragalá I. *J. Mater. Chem.*, **2003**,**13**:861-865

[4] Kim H, Park D W, Woo H C, et al. *Appl. Catal., B*, **1998**,**19**: 233-243

[5] Dong Y, He K, Yin L, et al. *Nanotechnology*, **2007**,**18**:435602-435607

[6] Morales A M, Lieber C M. *Science*, **1998**,**279**:208-211

[7] Lan X, Gao X, Qian W, et al. *J. Solid State Chem.*, **2007**,**180**: 2340-2345

[8] Liu X, Li C, Han S, et al. *Appl. Phys. Lett.*, **2003**,**82**:1950-1952

[9] Wang X, Chen X Y, Gao L S, et al. *J. Phys. Chem., B*, **2004**, **108**:16401-16404

[10]Gould J R, Lenhard J R, Muenter A A, et al. *J. Am. Chem. Soc.*, **2000**,**122**:11934-11943

[11]Jin R, Cao Y W, Mirkin A, et al. *Science*, **2001**,**294**:1901-1903

[12]Lai C H, Wu T F, Lan M D. *IEEE T Magn.*, **2005**,**41**:3397-3399

[13]Avgouropoulos G, Ioannides T. *Appl. Catal., B*, **2006**,**67**:1-2

[14]Luo M F, Ma J M, Lu J Q, et al. *J. Catal.*, **2007**,**246**:52-59

[15]Li D B, Liu X H, Zhang Q H, et al. *Catal. Lett.*, **2009**,**127**: 377-385

[16]Huang J, Wang S R, Zhao Y Q, et al. *Catal. Commun.*, **2006**,**7**: 1029-1034

[17]Sharma Y, Sharma N, Subba Rao G, et al. *J. Power Sources*, **2007**,**173**:495-501

[18]Tavares A C, Cartaxo M A M, Pereira M I D S, et al. *J. Solid State Electrochem.*, **2001**,**5**:57-67

[19]Dutta P, Seehra M S, Thota S, et al. *J. Phys. Condens. Matter.*, **2008**,**20**:1-8

[20]Wu S G, Zheng L Z, Rui L, et al. *Electroanalysis*, **2001**,**13**: 967-970